

Nematic Crossover in BaFe_2As_2 under Uniaxial Stress

Xiao Ren,¹ Lian Duan,¹ Yuwen Hu,¹ Jiarui Li,¹ Rui Zhang,² Huiqian Luo,³ Pengcheng Dai,² and Yuan Li^{1,4,*}

¹International Center for Quantum Materials, School of Physics, Peking University, Beijing 100871, China

²Department of Physics and Astronomy, Rice University, Houston, Texas 77005, USA

³Beijing National Laboratory for Condensed Matter Physics, Institute of Physics, Chinese Academy of Sciences, Beijing 100190, China

⁴Collaborative Innovation Center of Quantum Matter, Beijing 100871, China

(Received 8 July 2015; published 6 November 2015)

Raman scattering can detect spontaneous point-group symmetry breaking without resorting to single-domain samples. Here, we use this technique to study BaFe_2As_2 , the parent compound of the “122” Fe-based superconductors. We show that an applied compression along the Fe-Fe direction, which is commonly used to produce untwinned orthorhombic samples, changes the structural phase transition at temperature T_s into a crossover that spans a considerable temperature range above T_s . Even in crystals that are not subject to any applied force, a distribution of substantial residual stress remains, which may explain phenomena that are seemingly indicative of symmetry breaking above T_s . Our results are consistent with an onset of spontaneous nematicity only below T_s .

DOI: 10.1103/PhysRevLett.115.197002

PACS numbers: 74.25.nd, 74.25.Kc, 74.62.Fj, 74.70.Xa

In the phase diagram of iron-based superconductors, superconductivity is commonly situated near the vanishing point of the phase boundary between tetragonal and orthorhombic crystal structures [1–4]. This commonality has invoked major research efforts to elucidate the nature of the so-called nematic phase, in which the discrete C_4 rotational symmetry is lowered into C_2 but the lattice translational symmetry is intact. While the nematic phase is widely believed to be electronically driven, it is currently under debate whether the electrons’ spin or the orbital or charge degree of freedom is in the “driver’s seat” [5]. The fact that the tetragonal-to-orthorhombic structural phase transition is closely accompanied by a stripe antiferromagnetic order in the pnictides supports the spin-driven picture, whereas a pronounced uneven occupation of the Fe d_{xz} and d_{yz} orbitals in the orthorhombic phase [6–10] supports the orbital-driven picture. To accommodate the fact that FeSe possesses a nematic phase but no stripe antiferromagnetic order at ambient pressure, alternative scenarios for spin-driven nematicity which do not require long-range magnetic order [11–14] have also been proposed.

In order to address the driver’s seat question, it is important to study various susceptibilities in the tetragonal phase [5]. A prerequisite for such studies is precise knowledge about the onset temperature of spontaneous nematicity, T_{nem} and, in particular, whether T_{nem} is simply the orthorhombic structural transition temperature T_s —or even higher. The latter can be the case if spontaneous nematicity first develops electronically at T_{nem} with minor (although nonzero) influence on the crystal-lattice ground state, and at a lower temperature T_s , the lattice reaches a tipping point and responds strongly to the nematic electronic structure, bringing a pronounced C_2 signature to the entire system [15]. In such a scenario, experimental techniques that

directly probe the electrons are expected to reveal the nematicity in the temperature range $T_s < T < T_{\text{nem}}$.

Indeed, resistivity measurements have revealed a pronounced anisotropy in single crystals that are mechanically detwinned by pressing or pulling on one of the Fe-Fe directions [16–18]: the resistance along the compressed (elongated) direction becomes larger (smaller). This anisotropy is further found to persist to higher temperatures than T_s , an observation that has been attributed to either electronic nematic susceptibility [16,19], nematic fluctuations [17], or possible nematic transition or crossover above T_s [17,18]. In accordance with the resistivity anisotropy, spectroscopic evidence for a nematicity-related temperature range above T_s has also been reported, including anisotropic spin excitations seen by neutron scattering [20], C_2 -symmetric quasiparticle interference patterns seen by scanning tunneling spectroscopy [21], a gaplike feature seen by point-contact spectroscopy [22], and a splitting of the Fe d_{xz} and d_{yz} electronic bands seen by photoemission [6,9]. However, results of transport and thermodynamic measurements [23–28] do not support the existence of a well-defined phase transition at $T > T_s$, which implies that indications for $T_{\text{nem}} > T_s$ might be related to the application of a detwinning force on the crystals. A distinct piece of evidence for $T_{\text{nem}} > T_s$ came from magnetic torque measurements which revealed C_2 rather than C_4 symmetry above T_s [15]: the high sensitivity of the technique allows for measurements on tiny crystals which can be naturally dominated by one nematic domain without intentional detwinning. Still, however, the possible presence of residual stress in the crystals appears difficult to rule out. The debate on the precise relationship between T_{nem} and T_s persists into very recent studies [29–33], where the effect of applied and/or residual stress may be the

key to understanding some of the seemingly contradictory claims.

In order to verify the possible existence of spontaneous nematicity at $T > T_s$, and to elucidate the effect of external as well as residual stress on the phenomena related to C_4 -symmetry breaking, here we report a systematic study of phonon degeneracy in BaFe_2As_2 using Raman spectroscopy, with and without applied uniaxial stress. E_g phonons at the Brillouin-zone (BZ) center are doubly degenerate because of the global C_4 symmetry, and the lifting of such a degeneracy can be used to monitor the lowering of symmetry from C_4 to C_2 . Our method has four major advantages over transport and other spectroscopic measurements: (1) the Raman spectroscopic signature for C_4 -symmetry breaking is peak splitting and is unaffected by domain distribution; (2) our detection of lattice dynamics (rather than the equilibrium structure) is, in principle, also sensitive to nematic fluctuations; (3) the effect of applied force can be separately studied; and (4) the small laser-spot size allows us to gain insight into the local stress distribution. We find that a few MPa of applied uniaxial stress is sufficient to induce a nematic crossover that spans a wide temperature range above T_s , and that all our observations in “freestanding” samples, some of which could have been interpreted as evidence for $T_{\text{nem}} > T_s$, are in fact consistent with a distribution of residual stress on the same order of magnitude inside the crystals.

High-quality single crystals of BaFe_2As_2 were grown by a self-flux method [34]. At high temperature, the crystal structure belongs to the $I4/mmm$ space group and possesses two BZ-center E_g phonon modes, each of which is doubly degenerate and involves displacements of As and Fe atoms parallel to the ab plane. Without performing precise calculations, we schematically show their vibrational patterns in Fig. 1(a), from which one can see that the two modes are expected to have rather different energies: the low-energy mode involves half breathing of Fe-As plaquettes (shaded diamonds), whereas the high-energy mode involves full contraction and expansion of the plaquettes. The two modes have been previously identified by Raman spectroscopy [35] at about 130 and 270 cm^{-1} , respectively. At $T_s = 138$ K, the structure undergoes an orthorhombic transition which is closely accompanied by a magnetic phase transition [36,37], and in the orthorhombic phase each of the two E_g modes splits into a B_{2g} (slightly higher energy) and a B_{3g} (slightly lower energy) mode. Since the splitting of the low-energy E_g mode [Fig. 1(a)] is more pronounced [35], here we focus on the study of this mode only.

Our variable-temperature Raman scattering measurements were performed in a confocal backscattering geometry using a Horiba Jobin Yvon LabRAM HR Evolution spectrometer, equipped with 1800 gr/mm gratings and a liquid-nitrogen-cooled CCD detector. In order to achieve sufficiently high-energy resolution, we used the

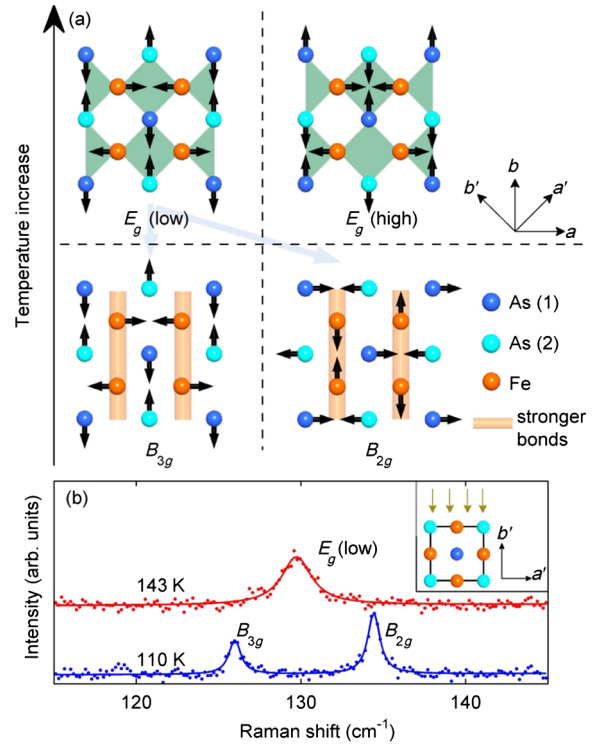


FIG. 1 (color online). (a) Vibrational patterns of two E_g phonons (the 90° rotated counterparts are not shown) in the tetragonal phase (the upper panels), along with those of B_{2g} and B_{3g} phonons in the orthorhombic phase (the lower panels) that derive from the low-energy E_g mode. (b) Raman spectra near the energy of the low-energy E_g mode peak above and below $T_s = 138$ K. (Inset) The Raman incident-light (arrows) geometry with respect to the crystal lattice.

$\lambda = 785$ nm line of a diode laser for excitation, and the laser power was set to 0.9 mW to reduce heating under the focal point which is about $5 \mu\text{m}$ in diameter. The sample temperature was controlled by a liquid-helium flow cryostat, with the sample kept under better than 5×10^{-8} Torr vacuum at all times. In order to best detect the E_g phonons, one of the incident and scattered light polarizations needs to be parallel to the c axis and the other to the ab plane, which requires measurements to be performed on a surface that is perpendicular to the ab plane, i.e., on the side of the platelike crystals. High-quality surfaces of this kind were obtained by cleaving the crystals right after freezing them in liquid nitrogen. To obtain high statistical precision, data acquisition for each spectrum took a minimum of 12 hours. A clear splitting of the low-energy E_g peak below T_s is demonstrated by the data displayed in Fig. 1(b).

Figure 2(a) displays Raman spectra measured at various temperatures with the incident and scattered photon polarizations parallel to the a' [Fig. 1(b) inset] and the c directions, which we denote as $(a'c)$ polarization for brevity. The sample was mounted by dipping its bottom into a droplet of viscous Apiezon N -type vacuum grease [Fig. 2(b) inset], which ensured good thermal contact but

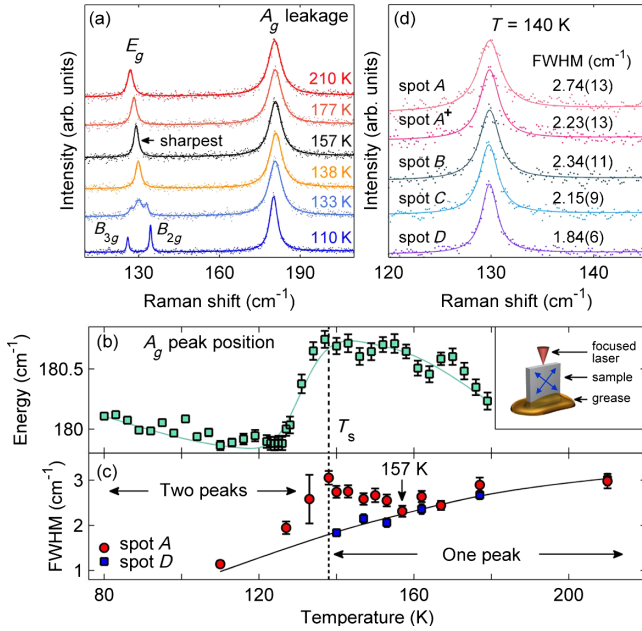


FIG. 2 (color online). (a) Raman spectra measured on a freestanding sample in $(a'c)$ -polarization geometry [see Fig. 1(a) for the axis definition] at various temperatures, offset for clarity. (b) T dependence of the A_g phonon energy determined from (cc) -polarization spectra obtained with the same laser power. (c) T dependence of the FWHM of the E_g ($T > T_s$) or B_{2g} and B_{3g} ($T < T_s$) peaks measured at two different surface locations specified in (d). The raw spectra were fitted with one Lorentzian peak above T_s (the vertical dashed line) and with two peaks below 132 K. The B_{2g} and B_{3g} peak width at T well below T_s is independent of the surface location. Solid lines in (b) and (c) are a guide for the eye. (d) Spectra measured in $(a'c)$ -polarization geometry at 140 K at four different surface locations, offset for clarity. Spot A^+ is the same location as A , but measured after a second cooling. The inset in (b) is a sketch of our sample geometry, with the Fe-Fe directions indicated by double-headed arrows.

applied only very little force onto the crystal. We hence refer to this sample as freestanding. Below T_s , the E_g phonon peak splits into B_{2g} and B_{3g} peaks, as has already been shown in Fig. 1(b), but, at 133 K immediately below T_s , a total of three peaks are observed. This can be attributed to laser heating, which we estimate to create a temperature distribution of ~ 5 K above the nominal temperature under the laser spot. Consistently, the A_g phonon energy measured with the same laser power but in (cc) polarization exhibits a pronounced anomaly that is shifted by about -8 K from the genuine T_s [Fig. 2(b)].

For regular phonons, their Raman peak widths are expected to decrease with decreasing temperature due to anharmonicity. A close inspection of the spectra above T_s in Fig. 2(a), however, indicates that the smallest full width at half maximum (FWHM) of the E_g phonon peak is realized not immediately above T_s , but around 157 K [“spot A” data in Fig. 2(c)]. It is tempting to interpret the anomalous broadening of the peak between 157 K and T_s as an

indication of onset of spontaneous nematicity above T_s , which might cause the E_g phonon to split into B_{2g} and B_{3g} peaks that are too close in energy to be individually resolved, or as a consequence of anomalous E_g phonon damping brought about by electronic nematic fluctuations. However, such interpretations are not supported by a careful investigation of the phenomenon at different sample-surface locations [Fig. 2(d)]: the spectra measured at 140 K at four different locations that are about $50 \mu\text{m}$ apart all show different linewidths; moreover, measurements performed at one of the same locations (A and A^+) but in different cooling cycles result in different linewidths beyond our measurement uncertainty. Finally, there is no anomalous broadening of the peak between 157 K and T_s at spot D , which exhibits the smallest FWHM at 140 K [Fig. 2(c)].

The above observations suggest an alternative, although relatively mundane, explanation for the anomalous broadening between 157 K and T_s , observed from spot A in Fig. 2: the effect could arise from the presence of nonuniform local residual stress, despite the fact that our sample was freestanding. Given the second-order nature of the structural transition at T_s , which is not particularly likely to give rise to residual stress, we speculate that residual stress may be induced by growth defects or our surface-preparation procedure. To explicitly examine the influence of stress, we performed a second set of measurements, with the sample mounted in the fashion shown in Fig. 3(a). By using an elastic BeCu sheet to press on the

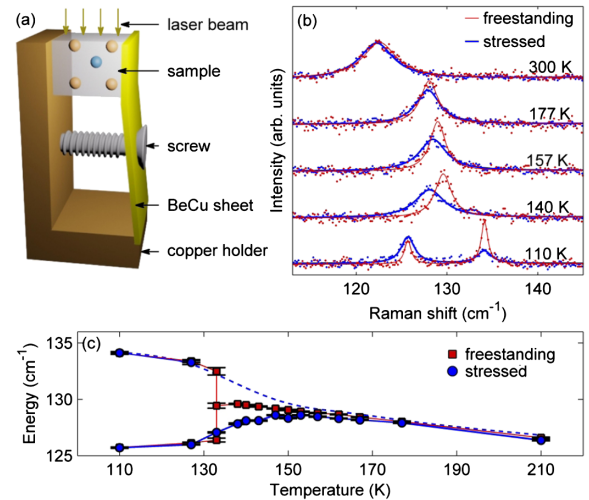


FIG. 3 (color online). (a) A schematic drawing of our sample mount that exerts a uniaxial compression along a Fe-Fe direction onto a crystal. (b) Comparison of Raman spectra at different temperatures measured on stressed and freestanding samples, under (ac) - and $(a'c)$ -polarization geometries, respectively, vertically offset for clarity. (c) T dependence of phonon energies in stressed and freestanding samples. Solid lines are a guide for the eye. Dotted line is an estimate of the B_{2g} phonon energy in the stressed sample, which we are unable to detect in the (ac) -polarization geometry.

crystal, an estimated 5 MPa of uniaxial compressive stress is introduced along one of the Fe-Fe directions, which is within a factor of 3 comparable to the amount of stress needed for complete sample detwinning [16,20]. A comparison of spectra obtained from stressed and freestanding samples is displayed in Fig. 3(b). At 110 K, the stressed sample exhibits a pronounced B_{3g} peak and only a weak B_{2g} peak, which is the opposite of the freestanding sample. This indicates that we have largely detwinned the crystal because our measurement of the stressed sample was carried out in the (bc) -polarization geometry, and in a fully detwinned sample we should not be able to detect the B_{2g} phonon at all.

According to the data in Fig. 3(b), while the uniaxial stress has only a minor effect on the peak positions above 160 K or below T_s , a large “shift” of the peak is found between 157 K and T_s . Because of the aforementioned reason pertaining to our polarization geometry, the peak shifted to lower energy in the stressed sample should be interpreted as one of two split peaks. Assuming that the other peak is symmetrically located on the high-energy side of the original E_g peak, the peak positions versus temperature in both freestanding and stressed samples are displayed in Fig. 3(c). Indeed, a rapid splitting of the phonon with cooling is found in the stressed sample below a similar temperature as the onset temperature $T \approx 157$ K for anomalous peak broadening in the freestanding sample. For a quantitative comparison, Fig. 4 displays both the peak shift in the stressed sample and the “extra” half width at half maximum (HWHM) of the peak in the freestanding sample, which would correspond to each other if the latter arises from the presence of two unresolvable peaks. In both cases, the data at $T > 140$ K can be reasonably well described by Landau’s theory, $\Delta E \propto (T - T_s)^{-1}$, and they are consistent with the trend of the diverging nematic susceptibility inferred both theoretically [38] and experimentally [19,26].

The comparison in Fig. 4 suggests that if the residual stress at spot *A* in Fig. 2 amounts to about one quarter that of our applied stress for the measurement in Fig. 3, it will be able to explain the anomalous broadening of the E_g phonon below 157 K. Such an amount of residual stress (1 to 2 MPa) is not unreasonable, as it may arise from processes of thermal cycling, mechanical polishing, and cleaving of the crystals, as well as from the presence of growth defects [39]. With a strongly reduced shear modulus near T_s [40], tiny residual stress can cause appreciable lattice deformation and change the structural phase transition into a crossover. Together with the nonuniform distribution of the E_g peak width at 140 K and the dependence on thermal cycling [Fig. 2(d)], our results provide rather strong evidence for a non-negligible influence of residual stress on the phenomena that are seemingly indicative of C_4 symmetry breaking above T_s . The results are consistent with a lack of genuine phase transition at $T > T_s$ inferred from transport and thermodynamic

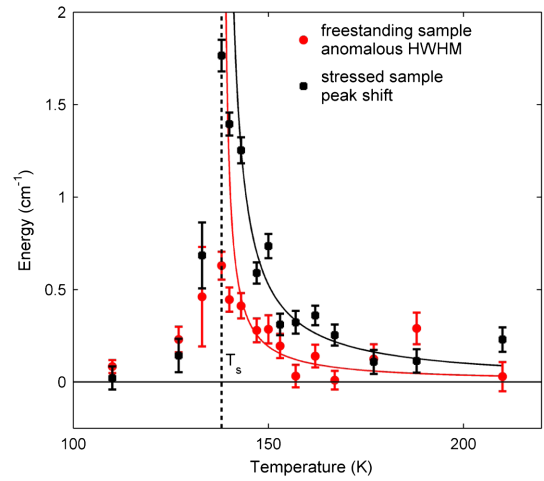


FIG. 4 (color online). Comparison between anomalous peak broadening in a freestanding sample (Fig. 2) and peak splitting (or shift) in a stressed sample (Fig. 3). The solid lines are fits according to Landau’s theory: $\Delta E \propto (T - T_s)^{-1}$.

measurements [23–28]. Indeed, at sample locations (spot *D* in Fig. 2) where residual stress is negligible, the intrinsic symmetry of the system is C_4 above T_s within our detection limit.

To conclude, our precise Raman scattering measurements of freestanding and stressed BaFe_2As_2 single crystals show that a moderate uniaxial stress on the order of a few MPa is sufficient to induce appreciable orthorhombicity in the system over a substantial temperature range above T_s . We further show that a hard-to-avoid distribution of residual stress on the order of 1 to 2 MPa is commonly present—even in nominally freestanding single crystals—with typical “domain” sizes comparable to or larger than the size of our laser spot ($\sim 5 \mu\text{m}$ in diameter). Interpretation of measurements done with detwinning forces applied to samples or on small sample volumes, therefore, needs to take these facts into account.

We wish to thank F. Wang, D.-H. Lee, A. Böhmer, D.-H. Lu, and Q.-M. Zhang for the stimulating discussions. The work at Peking University is supported by the NSF of China (Grant No. 11374024) and the NBRP of China (Grant No. 2013CB921903). The work at IOP, CAS, is supported by the NSF of China (Grant No. 11374011) and CAS (Grant No. SPRP-B: XDB07020300). The work at Rice University is supported by U.S. NSF Grants No. DMR-1362219 and No. DMR-1436006, and it is also supported in part by Robert A. Welch Foundation Grant No. C-1839 (P. D.).

* yuan.li@pku.edu.cn

- [1] D. C. Johnston, *Adv. Phys.* **59**, 803 (2010).
- [2] P. C. Canfield and S. L. Bud’ko, *Annu. Rev. Condens. Matter Phys.* **1**, 27 (2010).
- [3] J. Paglione and R. L. Greene, *Nat. Phys.* **6**, 645 (2010).

- [4] D. N. Basov and A. V. Chubukov, *Nat. Phys.* **7**, 272 (2011).
- [5] R. M. Fernandes, A. V. Chubukov, and J. Schmalian, *Nat. Phys.* **10**, 97 (2014).
- [6] M. Yi, D. Lu, J.-H. Chu, J. G. Analytis, A. P. Sorini, A. F. Kemper, B. Moritz, S.-K. Mo, R. G. Moore, M. Hashimoto, W.-S. Lee, Z. Hussain, T. P. Devereaux, I. R. Fisher, and Z.-X. Shen, *Proc. Natl. Acad. Sci. U.S.A.* **108**, 6878 (2011).
- [7] M. Yi, D. H. Lu, R. G. Moore, K. Kihou, C.-H. Lee, A. Iyo, H. Eisaki, T. Yoshida, A. Fujimori, and Z.-X. Shen, *New J. Phys.* **14**, 073019 (2012).
- [8] Y. Zhang, C. He, Z. R. Ye, J. Jiang, F. Chen, M. Xu, Q. Q. Ge, B. P. Xie, J. Wei, M. Aeschlimann, X. Y. Cui, M. Shi, J. P. Hu, and D. L. Feng, *Phys. Rev. B* **85**, 085121 (2012).
- [9] K. Nakayama, Y. Miyata, G. N. Phan, T. Sato, Y. Tanabe, T. Urata, K. Tanigaki, and T. Takahashi, *Phys. Rev. Lett.* **113**, 237001 (2014).
- [10] T. Shimojima, Y. Suzuki, T. Sonobe, A. Nakamura, M. Sakano, J. Omachi, K. Yoshioka, M. Kuwata-Gonokami, K. Ono, H. Kumigashira, A. E. Böhmer, F. Hardy, T. Wolf, C. Meingast, H. v. Löhneysen, H. Ikeda, and K. Ishizaka, *Phys. Rev. B* **90**, 121111 (2014).
- [11] F. Wang, S. Kivelson, and D.-H. Lee, *Nat. Phys.* (2015).
- [12] R. Yu and Q. Si, *Phys. Rev. Lett.* **115**, 116401 (2015).
- [13] J. K. Glasbrenner, I. I. Mazin, H. O. Jeschke, P. J. Hirschfeld, and R. Valenti, *Nat. Phys.* (2015).
- [14] A. V. Chubukov, R. M. Fernandes, and J. Schmalian, *Phys. Rev. B* **91**, 201105 (2015).
- [15] S. Kasahara, H. J. Shi, K. Hashimoto, S. Tonegawa, Y. Mizukami, T. Shibauchi, K. Sugimoto, T. Fukuda, T. Terashima, A. H. Nevidomskyy, and Y. Matsuda, *Nature (London)* **486**, 382 (2012).
- [16] J.-H. Chu, J. G. Analytis, K. De Greve, P. L. McMahon, Z. Islam, Y. Yamamoto, and I. R. Fisher, *Science* **329**, 824 (2010).
- [17] M. A. Tanatar, E. C. Blomberg, A. Kreyssig, M. G. Kim, N. Ni, A. Thaler, S. L. Bud'ko, P. C. Canfield, A. I. Goldman, I. I. Mazin, and R. Prozorov, *Phys. Rev. B* **81**, 184508 (2010).
- [18] J. J. Ying, X. F. Wang, T. Wu, Z. J. Xiang, R. H. Liu, Y. J. Yan, A. F. Wang, M. Zhang, G. J. Ye, P. Cheng, J. P. Hu, and X. H. Chen, *Phys. Rev. Lett.* **107**, 067001 (2011).
- [19] J.-H. Chu, H.-H. Kuo, J. G. Analytis, and I. R. Fisher, *Science* **337**, 710 (2012).
- [20] X. Lu, J. T. Park, R. Zhang, H. Luo, A. H. Nevidomskyy, Q. Si, and P. Dai, *Science* **345**, 657 (2014).
- [21] E. P. Rosenthal, E. F. Andrade, C. J. Arguello, R. M. Fernandes, L. Y. Xing, X. C. Wang, C. Q. Jin, A. J. Millis, and A. N. Pasupathy, *Nat. Phys.* **10**, 225 (2014).
- [22] H. Z. Arham, C. R. Hunt, W. K. Park, J. Gillett, S. D. Das, S. E. Sebastian, Z. J. Xu, J. S. Wen, Z. W. Lin, Q. Li, G. Gu, A. Thaler, S. L. Budko, P. C. Canfield, and L. H. Greene, *J. Phys. Conf. Ser.* **400**, 022001 (2012).
- [23] J.-H. Chu, J. G. Analytis, C. Kucharczyk, and I. R. Fisher, *Phys. Rev. B* **79**, 014506 (2009).
- [24] A. E. Böhmer, P. Burger, F. Hardy, T. Wolf, P. Schweiss, R. Fromknecht, M. Reinecker, W. Schranz, and C. Meingast, *Phys. Rev. Lett.* **112**, 047001 (2014).
- [25] X. Luo, V. Stanev, B. Shen, L. Fang, X. S. Ling, R. Osborn, S. Rosenkranz, T. M. Benseman, R. Divan, W.-K. Kwok, and U. Welp, *Phys. Rev. B* **91**, 094512 (2015).
- [26] A. E. Böhmer and C. Meingast, *C. R. Phys.* (2015).
- [27] A. E. Böhmer, P. Burger, F. Hardy, T. Wolf, P. Schweiss, R. Fromknecht, H. v. Löhneysen, C. Meingast, H. K. Mak, R. Lortz, S. Kasahara, T. Terashima, T. Shibauchi, and Y. Matsuda, *Phys. Rev. B* **86**, 094521 (2012).
- [28] C. Meingast, F. Hardy, R. Heid, P. Adelman, A. Böhmer, P. Burger, D. Ernst, R. Fromknecht, P. Schweiss, and T. Wolf, *Phys. Rev. Lett.* **108**, 177004 (2012).
- [29] H. Man, X. Lu, J. S. Chen, R. Zhang, W. Zhang, H. Luo, J. Kulda, A. Ivanov, T. Keller, E. Morosan, Q. Si, and P. Dai, *Phys. Rev. B* **92**, 134521 (2015).
- [30] X. Lu, T. Keller, W. Zhang, Y. Song, J. T. Park, H. Luo, S. Li, and P. Dai, Effect of uniaxial pressure on structural and magnetic phase transitions in electron-doped $\text{BaFe}_{2-x}\text{Ni}_x\text{As}_2$ superconductors, [arXiv:1507.04191](https://arxiv.org/abs/1507.04191).
- [31] Q. Deng, J. Liu, J. Xing, H. Yang, and H.-H. Wen, *Phys. Rev. B* **91**, 020508 (2015).
- [32] E. Thewalt, J. P. Hinton, I. Hayes, T. Helm, D. H. Lee, J. G. Analytis, and J. Orenstein, Optical evidence of broken C_4 symmetry across optimal doping in $\text{BaFe}_2(\text{As}_{1-x}\text{P}_x)_2$, [arXiv:1507.03981](https://arxiv.org/abs/1507.03981).
- [33] P. Cai, W. Ruan, X. Zhou, C. Ye, A. Wang, X. Chen, D.-H. Lee, and Y. Wang, *Phys. Rev. Lett.* **112**, 127001 (2014).
- [34] Y. C. Chen, X. Y. Lu, M. Wang, H. Q. Luo, and S. L. Li, *Supercond. Sci. Technol.* **24**, 065004 (2011).
- [35] L. Chauvière, Y. Gallais, M. Cazayous, A. Sacuto, M. A. Méasson, D. Colson, and A. Forget, *Phys. Rev. B* **80**, 094504 (2009).
- [36] M. Rotter, M. Tegel, D. Johrendt, I. Schellenberg, W. Hermes, and R. Pöttgen, *Phys. Rev. B* **78**, 020503 (2008).
- [37] M. G. Kim, R. M. Fernandes, A. Kreyssig, J. W. Kim, A. Thaler, S. L. Bud'ko, P. C. Canfield, R. J. McQueeney, J. Schmalian, and A. I. Goldman, *Phys. Rev. B* **83**, 134522 (2011).
- [38] S. Liang, A. Mukherjee, N. D. Patel, C. B. Bishop, E. Dagotto, and A. Moreo, *Phys. Rev. B* **90**, 184507 (2014).
- [39] P. J. Withers and H. K. D. H. Bhadeshia, *Mater. Sci. Technol.* **17**, 355 (2001).
- [40] M. Yoshizawa, D. Kimura, T. Chiba, S. Simayi, Y. Nakanishi, K. Kihou, C.-H. Lee, A. Iyo, H. Eisaki, M. Nakajima, and S.-i. Uchida, *J. Phys. Soc. Jpn.* **81**, 024604 (2012).